

# Spin-Fluctuation Mechanism of Superconductivity in Cuprates

A. Ramšak<sup>a,b</sup> and P. Prelovšek<sup>a,b</sup>

<sup>a</sup>Faculty of Mathematics and Physics, University of Ljubljana, Ljubljana, Slovenia;

<sup>b</sup>J. Stefan Institute, Ljubljana, Slovenia

## ABSTRACT

Normal and superconducting state spectral properties of cuprates are theoretically described within the extended  $t$ - $J$  model. The method is based on the equations of motion for projected fermionic operators and the mode-coupling approximation for the self-energy matrix. The dynamical spin susceptibility at various doping is considered as an input, extracted from experiments. The analysis shows that the onset of superconductivity is dominated by the spin-fluctuation contribution. The coupling to spin fluctuations directly involves the next-nearest-neighbor hopping  $t'$ , hence  $T_c$  shows a pronounced dependence on  $t'$ . The latter can offer an explanation for the variation of  $T_c$  among different families of hole-doped cuprates. A formula for maximum  $T_c$  is given and it is shown that optimum doping, where maximum  $T_c$  is reached, is with increasing  $-t'$  progressively increased.

**Keywords:** superconductivity, cuprates,  $t$ - $J$  model

## 1. INTRODUCTION

The mechanism of high-temperature superconductivity (SC) in cuprates represents one of the central open questions in the solid state theory. The role of strong correlations and the antiferromagnetic (AFM) state of the reference insulating undoped compound has been recognized very early.<sup>1</sup> Still, up to date there is no general consensus whether ingredients as embodied within the prototype single-band models of strongly correlated electrons are sufficient to explain the onset of high  $T_c$ , or in addition other degrees of freedom, as e.g. phonons, should be invoked. As the basis of our study, we assume the extended  $t$ - $J$  model,<sup>2</sup> allowing for the next-nearest-neighbor (NNN) hopping  $t'$  term. The latter model, as well as the Hubbard model,<sup>4</sup> both closely related in the strong correlation limit  $U \gg t$ , have been considered by numerous authors to address the existence of SC due to strong correlations alone. Within the parent resonating-valence-bond (RVB) theory<sup>1-3</sup> and slave-boson approaches to the  $t$ - $J$  model<sup>5</sup> the SC emerges due to the condensation of singlet pairs, induced by the exchange interaction  $J$ . An alternative view on strong correlations has been that AFM spin fluctuations, becoming particularly longer-ranged and soft at low hole doping, represent the relevant low-energy bosonic excitations mediating the attractive interaction between quasiparticles (QP) and induce the  $d$ -wave SC pairing. The latter scenario has been mainly followed in the planar Hubbard model<sup>4</sup> and in the phenomenological spin-fermion model.<sup>6</sup> Recent numerical studies of the planar  $t$ - $J$  model using the variational quantum Monte Carlo approach,<sup>7</sup> as well as of the Hubbard model using cluster dynamical mean-field approximation,<sup>8</sup> seem to confirm the stability of the  $d$ -wave SC as the ground state at intermediate hole doping. The relevance of  $t'$  for  $T_c$  has been already recognized<sup>9</sup> and recently, there are also some numerical studies of the influence of  $t'$  on pairing within prototype models,<sup>10,11</sup> although with conflicting conclusions.

## 2. MODEL AND METHOD

The  $t$ - $J$  model is nonperturbative by construction, so it is hard to design for it a trustworthy analytical method. One approach is to use the method of equations of motion (EQM) to derive an effective coupling between fermionic QP and spin fluctuations.<sup>12</sup> The latter method has been employed to evaluate the self energy and anomalous properties of the spectral function,<sup>12-14</sup> in particular the appearance of the pseudogap and the effective truncation of the Fermi surface (FS) at low hole doping.<sup>14</sup> The analysis has been extended to the study of the SC pairing,<sup>13,15</sup> while an analogous approach has been also applied to the Hubbard model.<sup>16</sup>

---

Further information: anton.ramsak@ijs.si

## 2.1. Equations of motion

We employ the formalism of the EQM and the resulting Eliashberg equations within the simplest mode-coupling approximation.<sup>13–15</sup> Equations involve the dynamical spin susceptibility which we consider as an phenomenological input taken from the inelastic-neutron-scattering (INS) and NMR-relaxation experiments in cuprates. The analysis of these experiments<sup>17</sup> reveals that in the metallic state the AFM staggered susceptibility is strongly enhanced at the crossover from the overdoped (OD) regime to optimum (OP) doping and is increasing further in underdoped (UD) cuprates, while at the same time the corresponding spin-fluctuation energy scale is becoming very soft. Direct evidence for the latter is the appearance of the resonant magnetic mode<sup>18,19</sup> within the SC phase indicating that the AFM paramagnon mode can become even lower than the SC gap. These facts give a support to the scenario that spin fluctuations in cuprates represent the lowest bosonic mode relevant for the  $d$ -wave SC pairing.

One of the central results of our EQM approach is that the relevant coupling to AFM paramagnons involves directly  $t'$ , but not  $t$ . The evident consequence is the sensitivity of  $T_c$  on  $t'$ , consistent with the experimental evidence for different families of cuprates.<sup>20</sup>

We consider the extended  $t$ - $J$  model

$$H = - \sum_{i,j,s} t_{ij} \tilde{c}_{js}^\dagger \tilde{c}_{is} + J \sum_{\langle ij \rangle} (\mathbf{S}_i \cdot \mathbf{S}_j - \frac{1}{4} n_i n_j), \quad (1)$$

including both the NN hopping  $t_{ij} = t$  and the NNN hopping  $t_{ij} = t'$ . The projection in fermionic operators,  $\tilde{c}_{is} = (1 - n_{i,-s})c_{is}$  leads to a nontrivial EQM, which can be in the  $\mathbf{k}$  basis represented as

$$\begin{aligned} [\tilde{c}_{\mathbf{k}s}, H] &= [(1 + c_h) \frac{\epsilon_{\mathbf{k}}^0}{2} - J(1 - c_h)] \tilde{c}_{\mathbf{k}s} + \\ &\frac{1}{\sqrt{N}} \sum_{\mathbf{q}} m_{\mathbf{kq}} [s S_{\mathbf{q}}^z \tilde{c}_{\mathbf{k}-\mathbf{q},s} + S_{\mathbf{q}}^\mp \tilde{c}_{\mathbf{k}-\mathbf{q},-s} - \frac{1}{2} \tilde{n}_{\mathbf{q}} \tilde{c}_{\mathbf{k}-\mathbf{q},s}], \end{aligned} \quad (2)$$

where  $c_h$  is the hole concentration and  $m_{\mathbf{kq}}$  is the effective spin-fermion coupling  $m_{\mathbf{kq}} = 2J\gamma_{\mathbf{q}} + \epsilon_{\mathbf{k}-\mathbf{q}}^0$ , while  $\epsilon_{\mathbf{k}}^0 = -4t\gamma_{\mathbf{k}} - 4t'\gamma'_{\mathbf{k}}$  is the bare band dispersion on a square lattice. We use the symmetrized coupling as derived in Ref. 14 to keep a similarity with the spin-fermion phenomenology<sup>6</sup>

$$\tilde{m}_{\mathbf{kq}} = 2J\gamma_{\mathbf{q}} + \frac{1}{2}(\epsilon_{\mathbf{k}-\mathbf{q}}^0 + \epsilon_{\mathbf{k}}^0). \quad (3)$$

EQM, Eq. (2), are used to derive the approximation for the Green's function (GF) matrix  $G_{\mathbf{k}s}(\omega) = \langle\langle \Psi_{\mathbf{k}s} | \Psi_{\mathbf{k}s}^\dagger \rangle\rangle_\omega$  for the spinor  $\Psi_{\mathbf{k}s} = (\tilde{c}_{\mathbf{k},s}, \tilde{c}_{-\mathbf{k},-s}^\dagger)$ .

## 2.2. Gap equation

We follow the method, as applied to the normal state (NS) GF by present authors,<sup>12,14</sup> and generalized to the SC pairing in Ref. 13. In general, we can represent the GF matrix in the form

$$G_{\mathbf{k}s}(\omega)^{-1} = \frac{1}{\alpha} [\omega\tau_0 - \hat{\zeta}_{\mathbf{k}s} + \mu\tau_3 - \Sigma_{\mathbf{k}s}(\omega)], \quad (4)$$

where  $\alpha = \sum_i \langle\langle \tilde{c}_{is}, \tilde{c}_{is}^\dagger \rangle\rangle_+ / N = (1 + c_h)/2$  is the normalization factor,  $\mu$  is the chemical potential and the frequency matrix,  $\hat{\zeta}_{\mathbf{k}s} = \frac{1}{\alpha} \langle\langle [\Psi_{\mathbf{k}s}, H], \Psi_{\mathbf{k}s}^\dagger \rangle\rangle_+$ , which generates a renormalized band  $\tilde{\zeta}_{\mathbf{k}} = \zeta_{\mathbf{k}s}^{11} = \bar{\zeta} - 4\eta_1 t\gamma_{\mathbf{k}} - 4\eta_2 t'\gamma'_{\mathbf{k}}$  and the mean-field (MF) SC gap

$$\Delta_{\mathbf{k}}^0 = \zeta_{\mathbf{k}s}^{12} = -\frac{4J}{N\alpha} \sum_{\mathbf{q}} \gamma_{\mathbf{k}-\mathbf{q}} \langle\tilde{c}_{-\mathbf{q},-s} \tilde{c}_{\mathbf{q},s}\rangle. \quad (5)$$

To evaluate  $\Sigma_{\mathbf{k}s}(\omega)$  we use the lowest-order mode-coupling approximation, analogous to the treatment of the SC in the spin-fermion model,<sup>6</sup> introduced in the  $t$ - $J$  model for the NS GF<sup>12,14</sup> and extended to the analysis of

the SC state.<sup>13</sup> Taking into account EQM, Eq. (2), and by decoupling fermionic and bosonic degrees of freedom, one gets

$$\Sigma_{\mathbf{k}s}^{11(12)}(i\omega_n) = \frac{-3}{N\alpha\beta} \sum_{\mathbf{q},m} \tilde{m}_{\mathbf{kq}}^2 G_{\mathbf{k}-\mathbf{q},s}^{11(12)}(i\omega_m) \chi_{\mathbf{q}}(i\omega_n - i\omega_m) \quad (6)$$

where  $i\omega_n = i\pi(2n+1)/\beta$  and  $\chi_{\mathbf{q}}(\omega)$  is the dynamical spin susceptibility, whereby we have neglected the charge-fluctuation contribution.

In order to analyze the low-energy behavior in the NS and in the SC state, we use the QP approximation for the spectral function matrix

$$A_{\mathbf{k}s}(\omega) \sim \frac{\alpha Z_{\mathbf{k}}}{2E_{\mathbf{k}}} (\omega\tau_0 - \epsilon_{\mathbf{k}}\tau_3 - \Delta_{\mathbf{k}s}\tau_1) [\delta(\omega - E_{\mathbf{k}}) - \delta(\omega + E_{\mathbf{k}})], \quad (7)$$

where  $E_{\mathbf{k}} = (\epsilon_{\mathbf{k}}^2 + \Delta_{\mathbf{k}s}^2)^{1/2}$ , while NS parameters, i.e., the QP weight  $Z_{\mathbf{k}}$  and the QP energy  $\epsilon_{\mathbf{k}}$ , are determined from  $G_{\mathbf{k}s}(\omega \sim 0)$ , Eq. (4). The renormalized SC gap is

$$\Delta_{\mathbf{k}s} = Z_{\mathbf{k}} [\Delta_{\mathbf{k}}^0 + \Sigma_{\mathbf{k}s}^{12}(0)]. \quad (8)$$

It follows from Eq. (4) that  $G_{\mathbf{k}s}^{12}(i\omega_n) \sim -\alpha Z_{\mathbf{k}} \Delta_{\mathbf{k}s} / (\omega_n^2 + E_{\mathbf{k}}^2)$ . By defining the normalized frequency dependence  $F_{\mathbf{q}}(i\omega_l) = \chi_{\mathbf{q}}(i\omega_l) / \chi_{\mathbf{q}}^0$ , and rewriting the MF gap, Eq. (5), in terms of the spectral function, Eq. (7), we can display the gap equation in a more familiar form,

$$\begin{aligned} \Delta_{\mathbf{k}s} = & \frac{1}{N} \sum_{\mathbf{q}} [4J\gamma_{\mathbf{k}-\mathbf{q}} - 3\tilde{m}_{\mathbf{k},\mathbf{k}-\mathbf{q}}^2 \chi_{\mathbf{k}-\mathbf{q}}^0 C_{\mathbf{q},\mathbf{k}-\mathbf{q}}] \times \\ & (Z_{\mathbf{k}}^0 Z_{\mathbf{q}}^0 \Delta_{\mathbf{q}s} / 2E_{\mathbf{q}}) \text{th}(\beta E_{\mathbf{q}} / 2), \end{aligned} \quad (9)$$

where  $C_{\mathbf{kq}} = I_{\mathbf{kq}}(i\omega_n \sim 0) / I_{\mathbf{k}}^0$  plays the role of the cutoff function with

$$I_{\mathbf{kq}}(i\omega_n) = \frac{1}{\beta} \sum_m F_{\mathbf{q}}(i\omega_n - i\omega_m) \frac{1}{\omega_m^2 + E_{\mathbf{k}s}^2}, \quad (10)$$

and  $I_{\mathbf{k}}^0 = \text{th}(\beta E_{\mathbf{k}} / 2) / (2E_{\mathbf{k}})$ . Eq. (9) represents the BCS-like expression which we use furtheron to evaluate  $T_c$ , as well as to discuss the SC gap  $\Delta_{\mathbf{q}}(T=0)$ . To proceed we need the input of two kinds: a) the dynamical spin susceptibility  $\chi_{\mathbf{q}}(\omega)$ , and b) the NS QP properties  $Z_{\mathbf{k}}, \epsilon_{\mathbf{k}}$ .

### 2.3. Parameters

The INS experiments show that within the NS the low- $\omega$  spin dynamics at  $\mathbf{q} \sim \mathbf{Q}$  is generally overdamped in the whole doping (but paramagnetic) regime.<sup>19</sup> Hence we assume  $\chi_{\mathbf{q}}(\omega)$  of the form

$$\chi_{\mathbf{q}}''(\omega) = \frac{B_{\mathbf{q}}\omega}{\omega^2 + \Gamma_{\mathbf{q}}^2}, \quad F_{\mathbf{q}}(i\omega_l) = \frac{\Gamma_{\mathbf{q}}}{|\omega_l| + \Gamma_{\mathbf{q}}}. \quad (11)$$

Following the recent memory-function analysis<sup>21</sup>  $B_{\mathbf{q}} = \chi_{\mathbf{q}}^0 \Gamma_{\mathbf{q}}$  should be quite independent of  $\tilde{\mathbf{q}} = \mathbf{q} - \mathbf{Q}$ . We choose the variation as  $\Gamma_{\mathbf{q}} \sim \Gamma_{\mathbf{Q}} (1 + w\tilde{q}^2/\kappa^2)^2$  consistent with the INS observation of faster than Lorentzian fall-off of  $\chi_{\mathbf{q}}''(\omega)$  vs.  $\tilde{q}$ .<sup>19</sup>  $w \sim 0.42$  in order that  $\kappa$  represents the usual inverse AFM correlation length.

Consequently, we end up with parameters  $\chi_{\mathbf{Q}}^0, \Gamma_{\mathbf{Q}}, \kappa$ , which are dependent on  $c_h$ , but in general as well vary with  $T$ . Although one can attempt to calculate them using the analogous framework,<sup>21</sup> we use here the experimental input for cuprates. We refer to results of the recent analysis,<sup>17</sup> where NMR  $T_{2G}$  relaxation and INS data were used to extract  $\kappa, \chi_{\mathbf{Q}}^0(T)$  and  $\Gamma_{\mathbf{Q}}(T)$  for various cuprates, ranging from the UD to the OD regime. For comparison with the  $t$ - $J$  model, we use usual parameters  $t = 400$  meV,  $J = 0.3t$ . At least for UD cuprates, quite consistent estimates for  $\chi_{\mathbf{Q}}^0, \Gamma_{\mathbf{Q}}$  can be obtained also directly from the INS spectra.<sup>19</sup> For UD, OP and OD regime, i.e.,  $c_h = 0.12, 0.17, 0.22$ , respectively, we use furtheron the following values:  $\chi_{\mathbf{Q}}^0 t = 15.0, 4.0, 1.0$ ,  $\Gamma_{\mathbf{Q}}^0 / t = 0.03, 0.1, 0.18$  (appropriate at low  $T$ ), and  $\kappa = 0.5, 1.0, 1.2$ . It is evident, that in the UD regime the energy scale  $\Gamma_{\mathbf{Q}}^0$  becomes very small (and consequently  $\chi_{\mathbf{Q}}^0 \propto 1/\Gamma_{\mathbf{Q}}^0$  large, in spite of modest  $\kappa^{17}$ ), supported by a pronounced resonance mode.<sup>19</sup> We take into account also the  $T$  dependence, i.e.,  $\Gamma_{\mathbf{Q}}(T) \sim \Gamma_{\mathbf{Q}}^0 + T$ ,<sup>17</sup> being significant only in the UD regime.

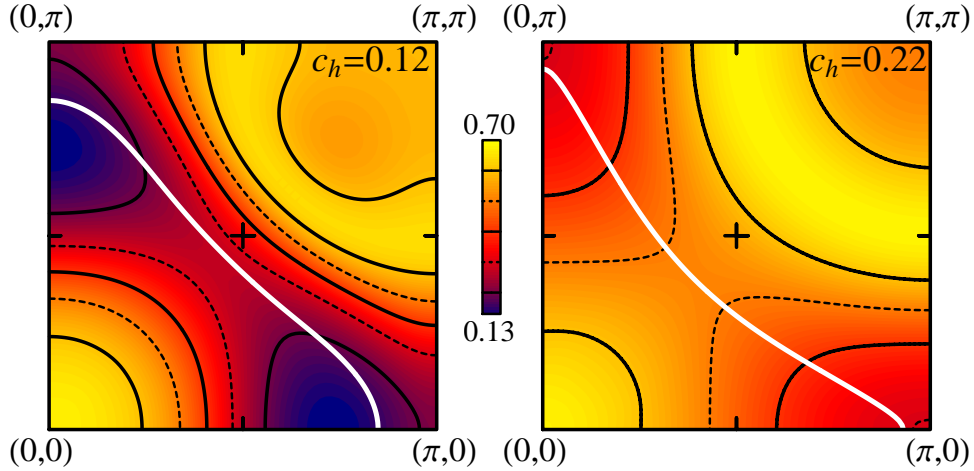


**Figure 1.** QP weight  $Z_{\mathbf{k}}$  evaluated for  $t'/t = -0.3$  for parameters corresponding to  $c_h = 0.12$  and  $c_h = 0.22$ , respectively. White line represents the location of the FS.

### 3. NUMERICAL RESULTS

#### 3.1. Normal state

For the NS  $A_{\mathbf{k}}(\omega)$  and corresponding  $Z_{\mathbf{k}}, \epsilon_{\mathbf{k}}$  we solve Eq. (6) for  $\Sigma_{\mathbf{k}}^{11} = \Sigma_{\mathbf{k}}$  as in Ref. 14, with the input for  $\chi_{\mathbf{q}}(\omega)$  as described above. Since our present aim is on the mechanism of the SC, we do not perform the full self-consistent calculation of  $\Sigma_{\mathbf{k}}(\omega)$ , but rather simplify it as done in the previous study.<sup>14</sup> Large incoherent  $\Sigma_{\mathbf{k}}(\omega \ll 0)$  leads to an overall decrease of the QP weight  $\bar{Z} < 1$  and the QP dispersion with renormalized  $\eta_1, \eta_2 < 1$ , which we assume here following Ref. 14, as  $\eta_1 = \eta_2 = 0.5, \bar{Z} = 0.7$ . Soft AFM fluctuations with  $\mathbf{q} \sim \mathbf{Q}$  lead through Eq. (6) to an additional reduction of  $Z_{\mathbf{k}}$ , which is  $\mathbf{k}$ -dependent. A pseudogap appears along the AFM zone boundary and the FS is effectively truncated in the UD regime with  $Z_{\mathbf{k}_F} \ll 1$  near the saddle points  $(\pi, 0)$  (in the antinodal part of the FS).<sup>14</sup> We fix  $\mu$  with the FS volume corresponding to band filling  $1 - c_h$ .

The coupling to low-energy AFM fluctuations, Eq. (6), leads to an additional QP renormalization. For fixed  $t'/t = -0.3$ , we present in Fig. 1 results for the variation of the  $Z_{\mathbf{k}}$  in the Brillouin zone for two sets of parameters, representing the UD and the OD regime, respectively. The location of the renormalized FS is also presented in Fig. 1. While the coupling to AFM fluctuations partly changes the shape of the FS, more pronounced effect is on the QP weight. It is evident from Fig. 1 that  $Z_{\mathbf{k}}$  is reduced along the AFM zone boundary away from the nodal points. Particularly strong renormalization  $Z_{\mathbf{k}} \ll 1$  happens in the UD case, leading to an effective truncation of the FS away from nodal points.<sup>14</sup>

#### 3.2. Superconducting state

First we comment on the general properties of the gap equation, Eq. (9). Close to half-filling and for  $\chi_{\mathbf{q}}^0$  peaked at  $\mathbf{q} \sim \mathbf{Q}$  both terms favor the  $d_{x^2-y^2}$  SC. The MF-part  $\Delta_{\mathbf{k}}^0$ , Eq. (5), involves only  $J$  which induces a nonretarded local attraction, playing the major role in the RVB theories.<sup>1,2</sup> In contrast, the spin-fluctuation part represents a retarded interaction due to the cutoff function  $C_{\mathbf{k}\mathbf{q}}$  determined by  $\Gamma_{\mathbf{k}-\mathbf{q}}$ . The largest contribution to the SC pairing naturally arises from the antinodal part of the FS. Meanwhile, in the same region of the FS also  $Z_{\mathbf{k}}$  is smallest, reducing the pairing strength in particular in the UD regime. Our analysis is also based on the lowest order mode-coupling treatment of the SC pairing as well as of the QP properties near the FS. Taking this into account, one can question the relative role of the hopping parameters  $t, t'$  and the exchange  $J$  in the coupling, Eq. (3). While our derivation within the  $t$ - $J$  model is straightforward, an analogous analysis within the Hubbard

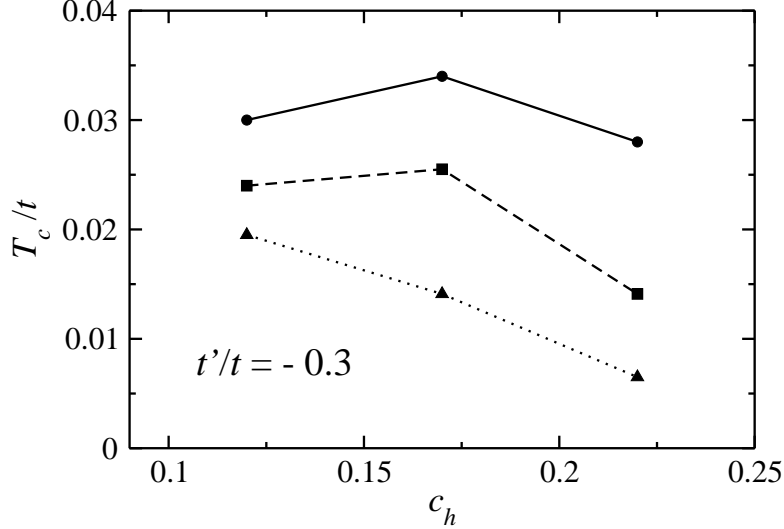


**Figure 2.**  $T_c/t$  vs. doping  $c_h$  for  $t'/t = -0.3$ , calculated for various versions of Eq. (9): a) full result (full line), b) with neglected MF term (dashed line), and c) in addition to b) modified  $\tilde{m}_{\mathbf{k}\mathbf{q}}$  without the  $J$  term (dotted line).

model using the projections to the lower and the upper Hubbard band, respectively, would not yield the  $J$  term within the lowest order since  $J \propto t^2$ . This stimulates us to investigate in the following also separately the role of  $J$  term in Eq. (9), both through the MF term, Eq. (5), and the coupling  $\tilde{m}_{\mathbf{k}\mathbf{q}}$ , Eq. (3).

NS results for  $Z_{\mathbf{k}}, \epsilon_{\mathbf{k}}$  are used as an input for the solution of the gap equation, Eq. (9), as presented in Fig. 2. For the same  $t'/t = -0.3$  we calculate  $T_c/t$  for  $c_h = 0.12, 0.17, 0.22$ . Besides the result a) of Eq. (9) (full line in Fig. 2) we present also two alternatives: b) the solution of Eq. (9) without the MF term, and c) the result with  $\tilde{m}_{\mathbf{k}\mathbf{q}}$  without the  $J$  term and omitted MF term. In the latter case, we used as input NS QP parameters, recalculated with correspondingly modified  $\tilde{m}_{\mathbf{k}\mathbf{q}}$ .

From Fig. 2 it is evident that the spin-fluctuation contribution is dominant over the MF term. When discussing the role of the  $J$  term in the coupling, Eq. (3), we note that in the most relevant region, i.e., along the AFM zone boundary  $\tilde{m}_{\mathbf{k}\mathbf{Q}} = 2J - 4t' \cos^2 k_x$ . Thus, for hole doped cuprates,  $t' < 0$  and  $J$  terms enhance each other in the coupling, and neglecting  $J$  in  $\tilde{m}_{\mathbf{k}\mathbf{q}}$  reduces  $T_c$ , although at the same time relevant  $Z_{\mathbf{k}}$  is enhanced.

The gap equation Eq. (9) leads to  $\Delta_{\mathbf{k}}$  with expected  $d_{x^2-y^2}$  symmetry form  $\Delta_{\mathbf{k}} \sim \Delta_0(\cos k_x - \cos k_y)/2$ , with  $\Delta_0(T=0) \sim \eta T_c$  and  $\eta \sim 2.5$ . However, we observe that in the UD regime the effective coherence length  $\xi \sim v_F/\Delta_0(T=0)$  becomes very short. I.e., with  $v_F$  taken as the average velocity over the region  $\kappa$  at the antinodal part of the FS we get  $\xi$  ranging from  $\xi = 4.4$  in the OD case, to  $\xi = 1.3$  in the UD example. In the latter case, SC pairs are quite local and the BCS-like approximation without phase fluctuations, Eqs. (9),(12), overestimates  $T_c$ . Starting from this side, a more local approach would be desirable. Full numerical solution of Eq. (9) is due to strong momentum dependent coupling also momentum dependent beyond the simple  $d$ -wave form. In Fig. 3(a)  $\Delta_{\mathbf{k}s}(T=0)$  is presented throughout the Brillouin zone for underdoped  $c_h = 0.12$  and coupling with emitted MF term as in (b) from Fig. 2 and for  $t'/t = -0.3$ . In the overdoped regime,  $c_h = 0.22$ , the momentum dependence of  $\Delta_{\mathbf{k}s}$  is less pronounced, Fig. 3(b), in accord with moderate momentum dependence of  $Z_{\mathbf{k}}$ , Fig. 1(b).

As discussed above, we take here the dynamical spin susceptibility independent of temperature, the approximation justified for low temperature  $T \sim T_c$  and solutions of the gap equation in the  $T < T_c$  regime should be considered only qualitatively. In Fig. 4 full temperature dependence of  $\Delta_{\mathbf{k}s}(T)$  is presented for  $\mathbf{k} = (\pi, 0)$  for various  $c_h$  and  $t'/t = -0.3$ . An interesting observation is increasing ratio  $\Delta_{(\pi,0)s}(T=0)/T_c$  from OD to UD regime reflecting different relative relevance of  $J$ - and  $t'$ -terms in the coupling.

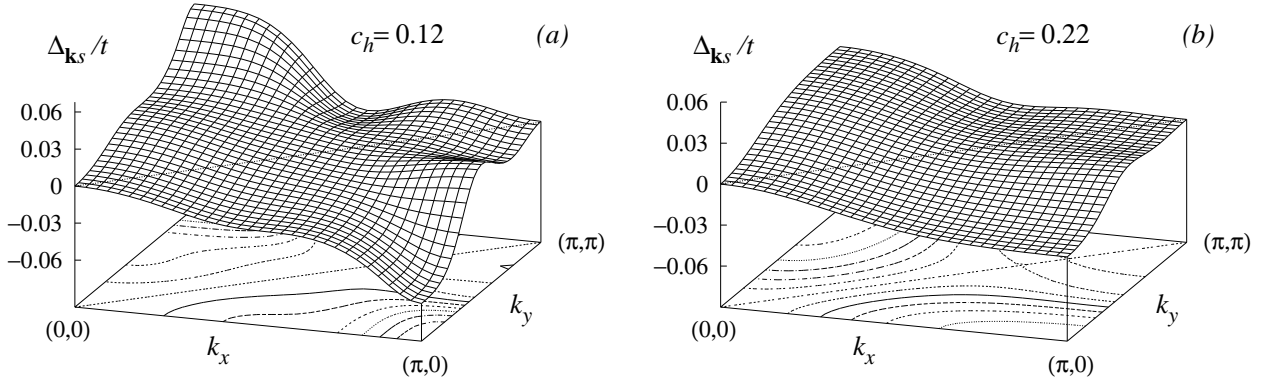


**Figure 3.** (a) Zero temperature  $\Delta_{\mathbf{k}_s}$  obtained from Eq. (9) using coupling without MF term [as in Fig. 2, line (b)], for  $c_h = 0.12$  and  $t'/t = -0.3$ . (b) As in (a), but for  $c_h = 0.22$ .

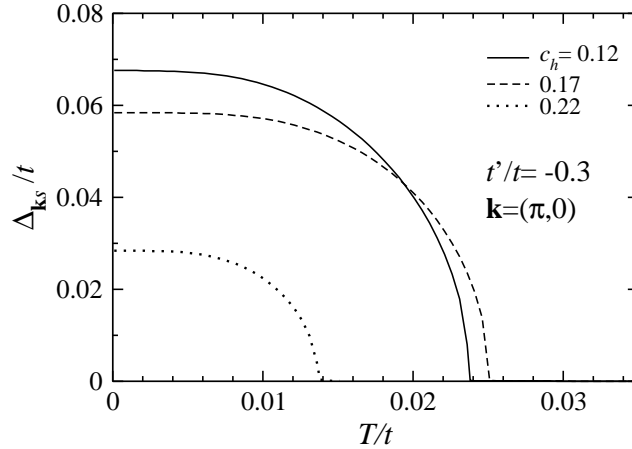


**Figure 4.** Temperature dependence of  $\Delta_{\mathbf{k}_s}(T)$  for  $\mathbf{k} = (\pi, 0)$  with parameters and coupling corresponding to Fig. 3.

Spin-fermion coupling  $\tilde{m}_{\mathbf{k}\mathbf{Q}}$  is strongly  $t'$ -dependent and as expected also  $T_c$  exhibits a pronounced dependence on  $t'/t$ . In Fig. 5 we present results, as obtained for fixed OP  $c_h = 0.17$ , but different  $t'/t < 0$ , as relevant for hole-doped cuprates.<sup>20</sup>

#### 4. DISCUSSION

Let us first comment on the relevance of the present method and results to cuprates. Our starting point is the model, Eq. (1), where strong correlations are explicitly taken into account via the projected fermionic operators. In this respect the derivation crucially differs from the analysis of the phenomenological spin-fermion model.<sup>6</sup> Nevertheless, in the latter approach the resulting gap equation, Eq. (9), looks similar but involves a constant effective coupling. In contrast, our  $\tilde{m}_{\mathbf{k}\mathbf{Q}}$ , Eq. (3), is evidently  $\mathbf{k}, \mathbf{q}$ -dependent. In particular, in the most relevant region, i.e., along the AFM zone boundary,  $\tilde{m}_{\mathbf{k}\mathbf{Q}}$  depends only on  $t'$  and  $J$ , but not on  $t$ . This explains our central result novel within the spin-fluctuation scenario, i.e., a pronounced dependence of  $T_c$  on  $t'$  which emerges directly via  $t'$  in the effective interaction in Eq. (12), and is consistent with the evidence from different families of cuprates.<sup>20</sup> Similar trend is obtained within the same model by the variational approach.<sup>11</sup> One can give

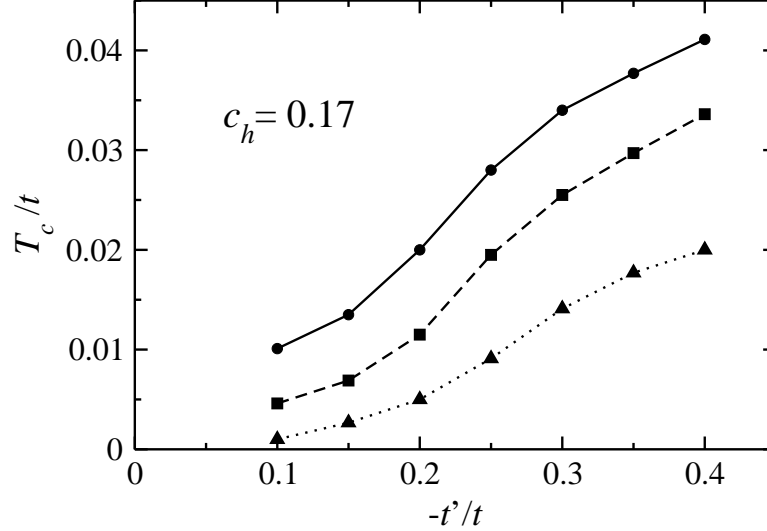


**Figure 5.**  $T_c/t$  vs.  $-t'/t$  for fixed 'optimum' doping  $c_h = 0.17$  and different versions of Eq. (9), as in Fig. 2.

a plausible explanation of this effect. In contrast to NN hopping  $t$ , the NNN  $t'$  represents the hopping within the same AFM sublattice, consequently in a double unit cell fermions couple directly to low-frequency AFM paramagnons, analogous to the case of FM fluctuations generating superfluidity in  $^3\text{He}$ .<sup>22</sup>

It is instructive to find an approximate BCS-like formula which simulates our results. The latter involves the characteristic cut-off energy  $\Gamma_{\mathbf{Q}}$ , while other relevant quantities are the electron density of states  $\mathcal{N}_0$  and  $Z_m$  being the minimum  $Z_{\mathbf{k}}$  on the FS (at the antinodal point). Then, we get a reasonable fit to our numerical results with the expression,

$$T_c \approx \frac{1}{2} \Gamma_{\mathbf{Q}} e^{-2/(\mathcal{N}_0 V_{eff})}, \quad (12)$$

where the effective interaction is given by  $V_{eff} = 3Z_m(2J - 4t')^2 \chi_{\mathbf{Q}}$ . Our numerical analysis suggests that the main  $t'$ -dependence of  $T_c$  originates in the coupling  $\tilde{m}_{\mathbf{k}\mathbf{q}}$ , not in  $\mathcal{N}_0 Z_m$ , while the main  $c_h$ -dependence comes from  $\chi_{\mathbf{Q}}$  and  $\Gamma_{\mathbf{Q}}$ . Then, Eq. (12) implies that optimum doping, where  $T_c$  reaches maximum, increases with  $-t'/t$ . For parameters used in Fig. 1, e.g.,  $c_{opt} = 0.13 + 0.12(-t'/t)$ .

In this analysis we do not extend our input data outside the doping range  $0.12 < c_h < 0.22$ . Nevertheless, we can discuss on the basis of Eq. (12) the variation  $T_c(c_h)$  elsewhere. Towards the undoped AFM also the spin fluctuation scale should vanish  $\Gamma_{\mathbf{Q}} \rightarrow 0$  and consequently  $T_c(c_h \rightarrow 0) \rightarrow 0$ . On the OD side,  $\chi_{\mathbf{Q}}$  and therefore  $V_{eff}$  should decrease with doping, leading again to fast reduction of  $T_c(c_h)$ .

It is evident from our analysis, that actual values of  $T_c$  are quite sensitive to input parameters and NS properties. Since we employ the lowest-order mode-coupling approximation in a regime without a small parameter, one can expect only a qualitatively correct behavior. Still, calculated  $T_c$  are in a reasonable range of values in cuprates. We also note that rather modest 'optimum'  $T_c$  value within presented spin-fluctuation scenario emerge due to two competing effects in Eqs. (9),(12): large  $\tilde{m}_{\mathbf{k}\mathbf{q}}$  and  $\chi_{\mathbf{Q}}$  enhance pairing, while at the same time through a reduced  $Z_{\mathbf{k}}$  and cutoff  $\Gamma_{\mathbf{Q}}$  they limit  $T_c$ .

It should also be noted that in the UD regime we are dealing with the strong coupling SC. Namely, we observe that  $\mathcal{N}_0 V_{eff}$  shows a pronounced increase at low doping mainly due to large  $\chi_{\mathbf{Q}}$ . Then it follows from Eq. (12) that  $T_c$  is limited and determined by  $\Gamma_{\mathbf{Q}}$ . At the same time, INS experiments<sup>19</sup> reveal that in the UD cuprates the resonant peak at  $\omega \sim \omega_r$  takes the dominant part of intensity of  $\mathbf{q} \sim \mathbf{Q}$  mode which becomes underdamped possibly even for  $T > T_c$ . Thus it is tempting to relate  $\Gamma_{\mathbf{Q}}$  to  $\omega_r$  (for more extensive discussion see Ref. 21) and in the UD regime to claim  $T_c \sim C\omega_r$ , indeed observed in cuprates<sup>19</sup> with  $C \sim 0.26$ . However, additional work is needed to accommodate properly an underdamped mode in our analysis.

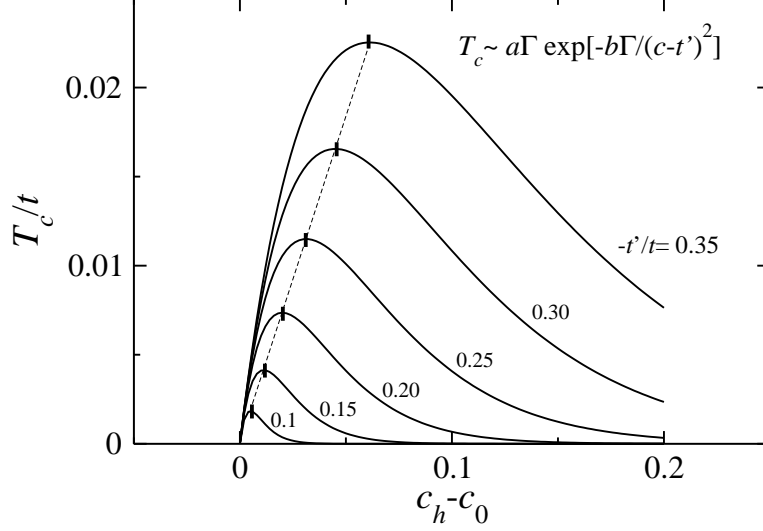


**Figure 6.**  $T_c$  vs.  $c_h$  with  $a\Gamma = (c_h - c_0)t$ ,  $b = 2at$  and  $c = 0$ . Dashed line connects the positions of  $T_{\max} = (c_{\text{opt}} - c_0)t/e$ .

Finally, let us conclude with a simplified qualitative picture emerging from our numerical analysis. As discussed above, full numerical treatment reproduces doping- and  $t'$ -dependence consistent with cuprates. NNN hopping matrix element  $t'$  enters the formalism in two ways. Firstly, through the dispersion of quasiparticles and corresponding renormalisation in NS leading to moderate increase of the density of states. Contrary to some other previous works, this effect is, surprisingly, not strongly doping dependent. More important is the effect of the spin-fermion coupling, where  $t'$  couples to spin susceptibility. The main  $t'$ -dependence of  $T_c$  comes from this part. The doping dependence emerges mainly due to strong spin susceptibility variation with  $c_h$ . Taking temperature independent  $\Gamma_{\mathbf{Q}}$  and  $\chi_{\mathbf{Q}} \propto \Gamma_{\mathbf{Q}}^{-1}$  together with the assumption of independence of the density of states on  $c_h$ , a simple qualitative formula for  $T_c$  emerges,

$$T_c = a\Gamma e^{-b\Gamma/(c-t')^2}. \quad (13)$$

As an example we take  $a\Gamma = (c_h - c_0)t$ ,  $b = 2at$  and we neglect spin exchange in the coupling,  $c = 0$ . In Fig. 5 doping dependence of such  $T_c$  is presented for various  $t'/t$ . In spite of severe approximations used in the derivation of Eq. (13), this result reflects the main features found also in the full numerical treatment: i)  $T_c$  is maximum in OP and decreasing in UD,OD regime, ii) larger maximum  $T_c$  at larger  $-t'$ , and iii) optimum  $c_{\text{opt}}$  increases with  $-t'$ . In the UD regime  $\Gamma$  is small compared to the relevant temperature scale and therefore for  $c_h \sim c_0$  the use of a more precise form of  $\Gamma(c_h, T)$  would be necessary. Maximum possible  $T_c$  based on Eq. (13) is given with  $T_{\max} = 0.37a\Gamma$ , where  $b\Gamma = (c - t')^2$  and therefore  $c_{\text{opt}} = c_0 + a(c - t')^2/(bt)$ .

Such estimates are consistent with our numerical results and could be relevant also for real cuprate materials. Maximum possible transition temperature is then given with approximate formula

$$T_{\max} \approx \frac{3}{4e} N_0 Z_m (2J - 4t')^2 \chi_{\mathbf{Q}} \Gamma_{\mathbf{Q}}. \quad (14)$$

## 5. ACKNOWLEDGEMENTS

Authors acknowledge stimulating discussions with N.M. Plakida and I. Sega. This research was supported by the Ministry of Higher Education and Science of Slovenia under grant P1-0044.



## REFERENCES

1. P. W. Anderson, "The resonating valence bond state in  $\text{La}_2\text{CuO}_4$  and superconductivity", *Science* **235**, 1196 (1987).
2. G. Baskaran, Z. Zou and P. W. Anderson, "The resonating valence bond state and high- $T_c$  superconductivity - a mean field-theory", *Solid State Commun.* **63**, 973 (1987).
3. C. Gros, R. Joynt, and T. M. Rice, "Superconducting instability in the large- $U$  limit of the two-dimensional Hubbard-model", *Z. Phys. B* **68**, 425 (1987).
4. N. Bulut, D. J. Scalapino, and S. R. White, "Comparison of Monte-Carlo and diagrammatic calculations for the 2-dimensional Hubbard-model", *Phys. Rev. B* **47**, 2742 (1993); D. J. Scalapino, "The case for  $d_{x^2-y^2}$  pairing in the cuprate superconductors", *Phys. Rep.* **250**, 330 (1995).
5. G. Kotliar and J. Liu, "Superexchange mechanism and d-wave superconductivity", *Phys. Rev. B* **38**, R5142 (1988); Y. Suzumura, Y. Hasegawa, and H. Fukuyama, "Mean field-theory of RVB and superconductivity", *J. Phys. Soc. Jpn.* **57**, 2768 (1988).
6. P. Monthoux and D. Pines, "YBa<sub>2</sub>Cu<sub>3</sub>O<sub>7</sub> - a nearly antiferromagnetic Fermi-liquid" *Phys. Rev. B* **47**, 6069 (1993); *Phys. Rev. B* **49**, 4261 (1994).
7. S. Sorella *et al.*, "Superconductivity in the two-dimensional t-J model", *Phys. Rev. Lett.* **88**, 117002 (2002).
8. Th. Maier, M. Jarrell, Th. Pruschke, and J. Keller, "d-wave superconductivity in the Hubbard model", *Phys. Rev. Lett.* **85**, 1524 (2000); T. A. Maier, M. Jarrell, A. Macridin, and C. Slezak, "Kinetic energy driven pairing in cuprate superconductors", *Phys. Rev. Lett.* **92**, 027005 (2004).
9. L. F. Feiner, J. H. Jefferson, and R. Raimondi, "Intrasublattice hopping in the extended t-J model and T-c(max) in the cuprates", *Phys. Rev. Lett.* **76**, 4939 (1996).
10. S. R. White, and D. J. Scalapino, "Competition between stripes and pairing in a t-t'-J model", *Phys. Rev. B* **60**, R753 (1999).
11. C. T. Shih, T. K. Lee, R. Eder, C.-Y. Mou, and Y. C. Chen, "Enhancement of pairing correlation by t' in the two-dimensional extended t-J model", *Phys. Rev. Lett.* **92**, 227002 (2004).
12. P. Prelovšek, "Electron Green's function in the planar t-J model", *Z. Phys. B* **103**, 363 (1997).
13. N. M. Plakida and V. S. Oudovenko, "Electron spectrum and superconductivity in the t-J model at moderate doping", *Phys. Rev. B* **59**, 11949 (1999).
14. P. Prelovšek and A. Ramšak, "Spectral functions and the pseudogap in the t-J model", *Phys. Rev. B* **63**, 180506(R) (2001); "Spectral functions, Fermi surface, and pseudogap in the t-J model", *ibid.* **65**, 174529 (2002).
15. P. Prelovšek and A. Ramšak, "Spin-fluctuation mechanism of superconductivity in cuprates", to appear in *Phys. Rev. B; cond-mat/0502044*.
16. S. Onoda and M. Imada, "Operator projection method applied to the single-particle Green's function in the Hubbard model", *J. Phys. Soc. Jpn.* **70**, 632 (2001).
17. J. Bonča, P. Prelovšek, and I. Sega, "Crossover to non-Fermi-liquid spin dynamics in cuprates", *Phys. Rev. B* **70**, 224505 (2004).
18. J. Rossat - Mignod *et al.*, "Neutron scattering study of the YBa<sub>2</sub>Cu<sub>3</sub>O<sub>6+x</sub>", *Physica C* **185-189**, 86 (1991).
19. H. F. Fong *et al.*, "Spin susceptibility in underdoped YBa<sub>2</sub>Cu<sub>3</sub>O<sub>6+x</sub>", *Phys. Rev. B* **61**, 14773 (2000); P. Dai, H. A. Mook, R. D. Hunt, and F. Dogan, "Evolution of the resonance and incommensurate spin fluctuations in superconducting YBa<sub>2</sub>Cu<sub>3</sub>O<sub>6+x</sub>", *Phys. Rev. B* **63**, 054525 (2001).
20. E. Pavarini, I. Dasgupta, T. Saha-Dasgupta, O. Jepsen, O. K. Andersen, "Band-structure trend in hole-doped cuprates and correlation with  $T_{cmax}$ ", *Phys. Rev. Lett.* **87**, 047003 (2001); K. Tanaka *et al.*, "Effects of next-nearest-neighbor hopping t on the electronic structure of cuprate superconductors", *Phys. Rev. B* **70**, 092503 (2004).
21. I. Sega, P. Prelovšek, and J. Bonča, "Magnetic fluctuations and resonant peak in cuprates: Towards a microscopic theory", *Phys. Rev. B* **68**, 054524 (2003); P. Prelovšek, I. Sega, and J. Bonča, "Scaling of the magnetic response in doped antiferromagnets", *Phys. Rev. Lett.* **92**, 027002 (2004).
22. A. J. Leggett, "A theoretical description of the new phases of liquid  $^3\text{He}$ ", *Rev. Mod. Phys.* **47**, 331 (1976).